Automated counting method for analyzing the results of *T. gondii* invasion assays

A Technical Report submitted to the Department of Biomedical Engineering

Presented to the Faculty of the School of Engineering and Applied Science

University of Virginia • Charlottesville, Virginia

In Partial Fulfillment of the Requirements for the Degree

Bachelor of Science, School of Engineering

Radhika Pande

Spring, 2022

Technical Project Team Members

Emma Wolcott

On my honor as a University Student, I have neither given nor received unauthorized aid on this assignment as defined by the Honor Guidelines for Thesis-Related Assignments

Brian Helmke, Department of Biomedical Engineering

Automated counting method for analyzing the results of *T. gondii* invasion assays

Radhika Pande and Emma Wolcott

Word count: 3775
Figures & Tables: 8
Equations: 1
Supplements: 0
References: 16

Advisor Signature: 

Abstract

Toxoplasma gondii is an obligate intracellular parasite that invades a wide variety of homeothermic hosts and can cause a disease called toxoplasmosis. The cost of this illness in the United States is estimated to be 3 billion dollars and an 11,000 quality-adjusted life-year loss annually. Approximately 8-22% of people in the United States are infected, and in most cases, the infection is asymptomatic. However, if a pregnant woman contracts toxoplasmosis, the child could develop blindness and intellectual disabilities, and the infection can even lead to death in immunocompromised people (Hill & Dubey, 2018). Toxoplasmosis is acquired through ingestion of tissue cysts in uncooked or undercooked meat or through ingestion of cat feces containing the parasite oocysts. The parasite invades by pulling itself into the host's gut epithelial cells, but the proteins involved in this process have not fully been identified. This process may involve a force balance between the parasite and the host cell that involves the host cell's cytoskeleton. The cytoskeletal morphology and stiffness of a cell can be manipulated by plating the cell on substrates of varying stiffnesses, in this case polyacrylamide (PA) gels with three ranges of stiffness as well as glass substrates (Yeung et al., 2005). Invasion assays were used to quantify the number of parasites that invade host cells on the different substrates and it was found that substrate stiffness may affect the invasion of wild type *T. gondii* parasites but not parasites with SPM1, TLAP3, and TLAP4 knocked out. The output of the invasion assay is fluorescent images which must be analyzed with a process that is both time-efficient and accurate. An image analysis workflow was designed using CellProfiler and the results were found to not be statistically different from manual counts.

Key words: *Toxoplasma gondii*, toxoplasmosis, polyacrylamide, CellProfiler

Introduction

Toxoplasma gondii is an intracellular parasite transmitted to humans through contaminated food or cat feces. In the United States, approximately 11% of the population six years and older are infected with the parasite, and this number is as high as 60% in some regions of the world. In most cases of infection, the host's immune system is able to prevent the parasite from causing illness, but in immunocompromised people and pregnant women, infection by *T. gondii*, called toxoplasmosis, can be very serious. The CDC considers toxoplasmosis to be one of the five neglected parasitic infections in the United States and has targeted it for public health action (*CDC - Toxoplasmosis*, 2021).

When a pregnant woman is infected by *T. gondii*, she can pass the infection to her unborn child through the placenta. This can potentially result in a miscarriage, a stillborn child, or a child born with signs of congenital toxoplasmosis. *T. gondii* infection can also cause eye disease, most often retinochoroiditis, the symptoms of which include eye pain, sensitivity to light, tearing of the eyes, and blurred vision. Toxoplasmosis is also dangerous for people with compromised immune systems, as infection can result in brain-occupying lesions, encephalitis, pneumonia, fever, severe sepsis, and other symptoms, and can lead to death (Montoya & Contopoulos-Ioannidis, 2021). Treatment of toxoplasmosis involves a combination of drugs such as pyrimethamine and sulfadiazine, but these do not completely eliminate parasites in the tissue, so symptoms can persist and medication may need to be taken for the rest of one's life (*CDC - Toxoplasmosis*, 2021). In order to develop better treatments for toxoplasmosis, the method of *T. gondii* invasion must be better understood.

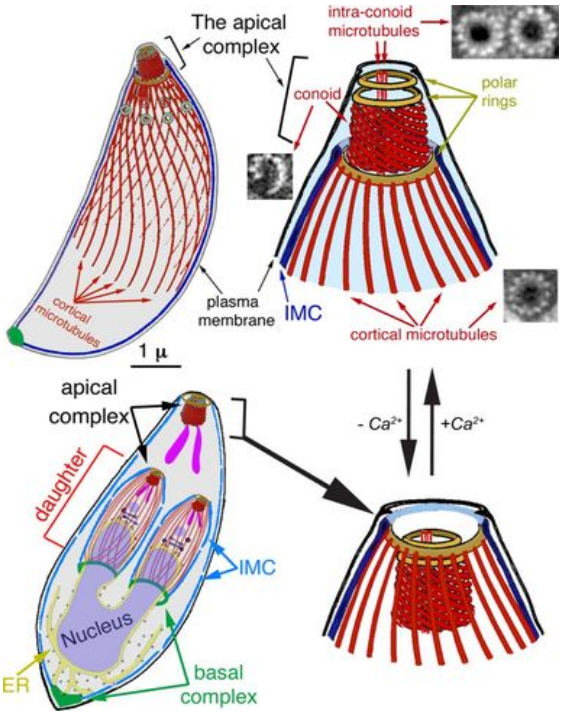

Figure 1. Diagrams of the *T. gondii* cytoskeleton. This figure displays several tubulin-containing structures in the *T. gondii* parasite, including electron microscopic cross-sections of the cortical and intraconoid microtubules and a conoid fiber. The bottom left image displays the replication of a parasite into daughter parasites. The bottom right image provides a more detailed look at the structure of the apical complex at the tip of the parasite. From Liu et al.

The structure of *T. gondii* consists of at least five different types of tubulin-based structures, which contribute to the integrity of the parasite as well as its ability to invade and proliferate (Figure 1). The parasite is one of around 6,000 parasites in the phylum Apicomplexa, related closely to the notorious malarial parasite *Plasmodium* spp. Invasion mechanisms for both parasites are similar, wherein the parasite penetrates the host cell membrane, establishes vacuoles in the host, proliferates rapidly, escapes from the now resource-depleted host, and then disseminates to initiate invasion in other cells. The invasion is mature once the parasite has replicated enough times to form a rosette structure, connected by a singular residual body in the center.

T. gondii invades host cells by actively pulling itself in, and it has been hypothesized that the force needed for this motion comes from the parasite's interaction with the host cell cytoskeleton. The interface between the invading parasite and the host cell is called the moving junction (MJ), and it serves as an anchor and entry point into the cell. The proteins needed to form the MJ are secreted from the parasite's microneme and rhoptry organelles and interact with host cell proteins to form a complex. These host cell proteins in turn interact with the actin cytoskeleton, which allows the parasite to use the host cell cytoskeleton as an anchor for invasion (Guérin et al., 2017). Therefore, the integrity of the host cell cytoskeleton is important for the ability of *T. gondii* to invade.

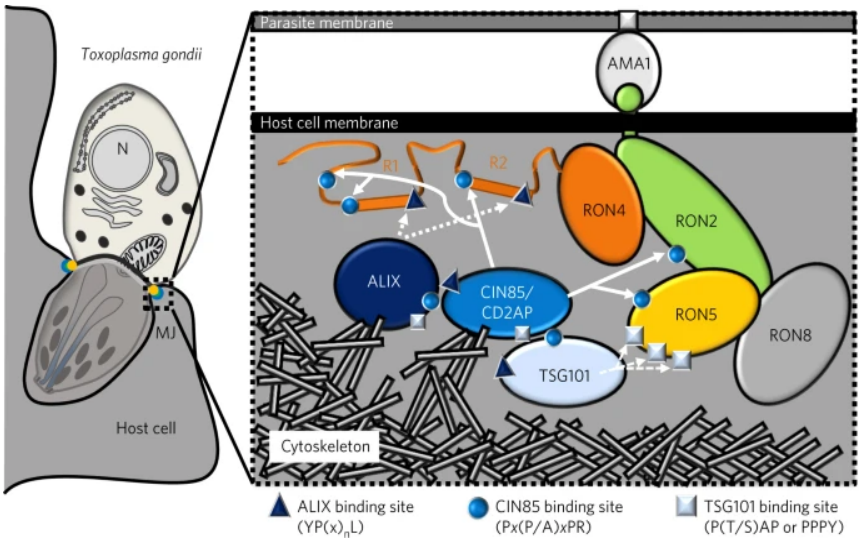

Figure 3. Proteins involved in forming the moving junction.
Proteins secreted from the parasite's rhoptry and microneme organelles (AMA1, RON) interact with host cell proteins (TSG101, CIN85/CD2AP) which in turn interact with proteins that are associated with host cell actin (ALIX). This complex allows the protein to anchor itself to the host cell cytoskeleton. From Guerin et al., 2017

Cytochalasin D (CD) is a drug that disrupts the F-actin structure in the cytoskeleton, therefore treating cells with the drug makes them "floppier" and there is less of a force for parasites to pull themselves against to gain entry into the host cell. It was found that putting CD into the medium of both phagocytic and non-phagocytic cells decreased *T. gondii* invasion, suggesting that the host cell cytoskeleton plays a role in invasion (Ryning & Remington, 1978). A separate experiment found that invasion was blocked when CD-resistant host cells were treated with CD, which would disrupt the parasite's actin, while invasion was not affected by treatment of CD-resistant parasites with CD, which would disrupt the host cell's actin. This suggests the host cell cytoskeleton is not involved in invasion, but that invasion is powered by an actin-based contractile system in the parasite (Dobrowolski & Sibley, 1996). Yet another experiment demonstrated that treatment of host cells with CD decreased parasite invasion, and they confirmed that the effects of CD were mainly on host cell actin rather than parasite actin (Silva et al., 2009). These conflicting results demonstrate the gap in knowledge about the role of the host cell cytoskeleton in *T. gondii* invasion.

In the body, cells interact with the extracellular matrix (ECM), and these interactions influence cell migration, differentiation, and morphology. The ECM can be modeled *in vitro* with protein-coated hydrogels, and cells can be plated on these gels in order to investigate changes in their functions and morphology. Polyacrylamide (PA) gels can be formulated to have different stiffnesses by using varying concentrations of acrylamide and bis-acrylamide, and the stiffness of the gels affects the properties of the cells plated on them. When fibroblasts were plated on PA gels with stiffnesses ranging from 180 Pa to 16,000 Pa, it was found that the cells on soft gels had no actin stress fibers compared to cells on the stiff gels. Cell circumference, cell area, and spreading rate were also found to be greater on stiffer gels than on softer ones (Yeung et al., 2005). Cell traction force also increases with increasing gel stiffness and cell-substate adhesions on soft gels are dynamic while these adhesions are static on stiff gels (Discher et al., 2005). Atomic force microscopy was used to measure the stiffness of fibroblasts on PA gels with a range of moduli, and it was found that cells were stiffer and had greater amounts of cross-linked F-actin on the stiffer gels (Solon et al., 2007). Overall, these results demonstrate that a cell's cytoskeletal morphology and stiffness are dependent on the stiffness of the substrate it is on, and this can be used to easily manipulate the cytoskeleton.

In order to investigate whether the host cell cytoskeleton is involved in invasion, *T. gondii* invasion of cells plated on PA gel substrates with three different stiffnesses was measured. As described above, cytoskeletal morphology and stiffness is affected by the stiffness of the substrate on which the cells are plated. Therefore, if the host cell cytoskeleton is involved in invasion, the number of parasites that invade the host cells on substrates of different stiffnesses should differ. This method was also performed using *T. gondii* parasites with the proteins SPM1, TLAP3, and TLAP4 knocked out. SPM1 is found along

the entire length of the parasite's cortical microtubules while TLAP3 and TLAP4 are differentially distributed along the polymers. These proteins protect the stability of the cortical microtubules and it has been shown that a triple knockout of these proteins leads to significantly decreased invasion when compared to wild type parasites (Liu et al., 2016). If different amounts of invasion on different substrates are observed for the wild type (WT) and triple knockout (TKO) parasites, it could be concluded that these proteins are not involved in host-cell cytoskeleton-dependent invasion. However, if the pattern is different between the wild type and triple knockout parasites, it may indicate that the three proteins do play a role in detecting or manipulating the host cell cytoskeleton.

The invasion assays produce large quantities of data, an estimated 8,000 objects per experiment, that must be counted in order to obtain the results. Doing this by hand takes around two hours for one person to do, and often multiple people have to count the same images in order to verify the results, which adds to the amount of labor needed. In order to analyze these results more efficiently while getting the same results as manual counts, we designed an automated counting workflow in CellProfiler. Our goal was to halve the time needed to perform the analysis while yielding results that were equally as accurate as manual counts.

Materials and Methods

Polyacrylamide gel production

The protocol for the production of polyacrylamide gels was modified from Paszek et al.. The first step was to soak square 22x22 mm glass coverslips in Sparklene overnight, rinse them with distilled water for 15 minutes, then autoclave them. The next step was glass functionalization, which consisted of pipetting 200 µL of 0.1M NaOH onto the coverslips, then incubating them at room temperature for five minutes. The coverslips were dried with vacuum aspiration, and 200 µL APTMS was pipetted on, followed by another five-minute incubation. The coverslips were rinsed by trickling water over them, then washed three times with distilled water, with five minutes between each wash. Then 200 µL of 0.5% glutaraldehyde was pipetted on, and the coverslips were incubated for 30 minutes at room temperature and washed in the same manner as above. The liquid was then aspirated off and the coverslips were left to air-dry overnight.

The next step was to formulate the polyacrylamide (PA) gel solutions on the coverslips. The PA gel solutions were made of 30% acrylamide stock solution, 1% bis stock solution, and distilled water. The solutions were formulated as follows: 3% acrylamide and 0.06% bis-acrylamide for soft, 5% acrylamide and 0.3% bis-acrylamide for medium, and 10% acrylamide and 0.6% bis-acrylamide for stiff. The solutions were combined in a tube and de-gassed for 15 minutes in a desiccator. After this, the polymerization solutions were prepared by combining 2 mL of polyacrylamide solution, 10 µL of APS solution (0.1 g APS and 0.9 mL water), and 2 µL TEMED. 45 µL of polymerization solution was pipetted onto each coverslip and sandwiched under a circular 18x18 mm coverslip. The gels were left to polymerize for 60 minutes, then the top coverslip was removed with a hook formed from the tip of a bent needle.

If the PA gels were used for cell-plating, they were then coated with type I collagen. First, the gels were washed three times with 50 mM HEPES pH 8.5, with five-minute incubations. Then 200 µL of a 20% sulfo-SANPAH solution in HEPES was pipetted onto each gel and incubated under UV light for 20 minutes. The gels were again washed three times with HEPES, then 2 mL of a 0.2 mg/mL collagen solution was pipetted onto each gel, and the coverslips were incubated overnight at 4°C.

Polyacrylamide gel stiffness testing

An Optics 11 nanoindenter was used to characterize the elastic modulus of the PA gels. The method of nanoindentation involved lowering a probe into the surface of the sample and recording the load and displacement, yielding a load-displacement, or stress-strain curve as seen in Figure 3. For soft materials, such as PA gels, the Hertz model is the most suitable method of fitting the data and deriving an elastic modulus. The Hertz model utilizes the loading portion of the load-displacement curve and the elastic modulus is derived as Equation 1:

$$E = \frac{3(1-\upsilon^2)P}{4R^{\frac{1}{2}}h^{\frac{3}{2}}} \quad [1]$$

where ν is the Poisson's ratio, P is the load, R is the radius of the spherical indenter tip, and h is the indentation depth. Over 400 measurements on each gel stiffness were performed in order to establish consistency across measurements on gels made on different days.

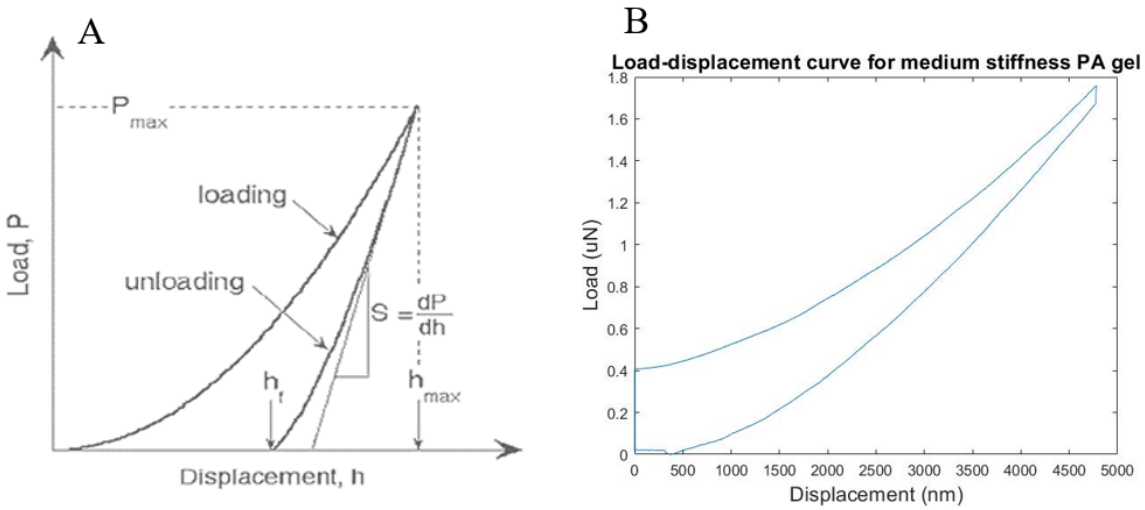

Figure 3. Load-displacement curves. (A) The Hertz model fits a line to the loading portion of the curve. Taken from Mattei et al. (B) Example of a load-displacement curve generated from nanoindenter measurements on a medium stiffness PA gel.

Plating cells on gels

Human foreskin fibroblasts (HFFs) were cultured in growth medium made up of 10% heat-inactivated calf serum (HINCS), 1% sodium pyruvate, 1% L-glutamine, and 88% DMEM. HFFs were plated on PA gels in the following manner. First, the medium was aspirated off and the cells were rinsed with PBS -/-. The PBS was aspirated off and 1.5 mL of trypsin-EDTA was added, followed by an incubation at 37°C for three minutes. 7.5 mL of growth medium was then added to stop trypsinization and the cells were transferred to a 15 mL centrifuge tube. The cells were centrifuged for five minutes at 250 g and 4°C, then the supernatant was removed and the pellet was resuspended in 10 mL of growth medium. A hemocytometer was used to count the number of cells per mL, and the calculated volume of cells was pipetted onto each PA gel in order to have $4x10^4$ cells/cm^2. A 35 mm glass MatTek dish was used as a control alongside the PA gels with density $2x10^4$ cells/cm^2. The plated cells were left in the incubator for 36-48 hours to allow them time to adhere to and spread on the substrate.

T. gondii invasion assay

To quantify the invasion of the parasite *Toxoplasma gondii*, an invasion assay was performed using host cells on PA gel substrates of three different stiffnesses. The first step was staining the nuclei of the host cells with bisBenzamide to allow for automatic cell counting later on. Then, the host cells were infected with *T. gondii* tachyzoites at a concentration of $1x10^7$ tachyzoites/mL, and the invasion was allowed to proceed for one hour. After one hour, the host cells and parasites were fixed with 4% paraformaldehyde, followed by a 20-minute incubation with 1% bovine serum albumin (BSA) to block nonspecific binding. The following antibody incubations were with antibodies in a 1:1000 dilution with BSA for 30 minutes. Next was labeling with a primary antibody (rabbit α-P30) that binds to TgSAG1, a *T.*

gondii surface antigen, followed by a secondary antibody (goat α-rabbit Alexa 594). This antibody labeling only labeled parasites that had not invaded the host cells (extracellular). The host cell membrane was then permeabilized with 0.5% Triton X-100 for 15 minutes and the parasites were again labeled with a primary antibody that binds to TgSAG1 followed by a secondary antibody (goat α-rabbit Alexa 488). This labeled both the parasites that had not invaded (extracellular) and the parasites that had invaded (intracellular). The coverslips were mounted on slides and imaged using confocal microscopy. A TRITC filter was used to image the parasites labeled with Alexa 594 and a FITC filter was used to image the parasites labeled with Alexa 488. In order to calculate the number of parasites that invaded, the number of extracellular parasites was subtracted from the total number of parasites.

Automated counting method

CellProfiler was used for the design of an automated counting of parasites in the images resulting from the invasion assays. The six steps of the workflow are summarized in Figure 4.

The first input to the workflow is the FITC or TRITC image that contains the fluorescently labeled parasites. In order to minimize the amount of autofluorescence that could be detected as parasites, the noise was reduced using a patch size of 5 pixels, a maximum distance to search for patches to use for denoising of 7 pixels, and a cut-off distance of 0.1 pixels (Figure 4A and B). The reduced noise image was then used to identify objects. The typical diameter of the objects was set as 5-45 pixels and the Otsu method was used to threshold the image. The objects in this image were then filtered using a mean radius range of 3-7 pixels and a mean intensity range of 0.15-2 (Figure 4C and D). In the next module, the objects were manually edited in order to separate any objects that had been identified as one object but were actually two or more (Figure 4E and F). Finally, the outlines of the objects were overlaid on the original image and the number of objects per image was saved to a spreadsheet.

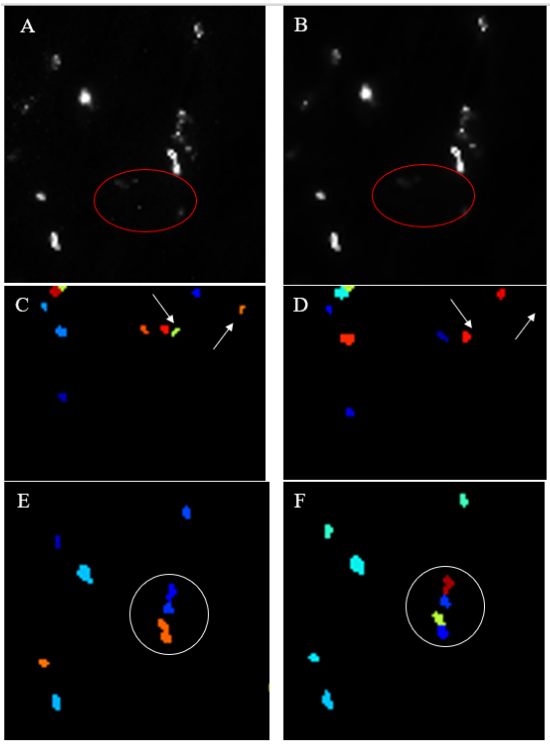

Figure 4. Automated counting workflow method
(A and B) Remove noise. The red circles indicate an area where there was noise in the original image (A) which was removed in B.
(C and D) Filter objects. The arrows point to objects that were filtered by size and intensity.
(E and F). Edit objects manually. The circles indicate two objects in E that were separated in F.

Results

Polyacrylamide gel stiffness testing

An Optics11 nanoindenter was used to measure the elastic modulus of soft, medium, and stiff polyacrylamide gels. Indentations were performed in a three-by-three matrix spaced 200 micrometers apart and three of these matrix scans were done on each gel in different locations on the gel. The measurements were taken over eight days and a new batch of gels was used on each day. The results of using nanoindentation to measure polyacrylamide gel stiffness are summarized in Figure 5.

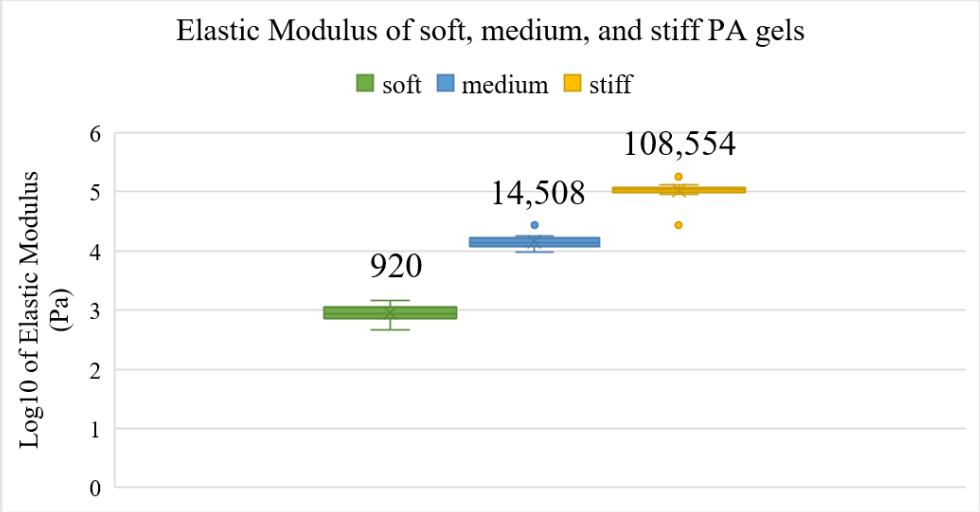

Figure 5. Elastic modulus measurements on polyacrylamide gels of three stiffnesses. The elastic moduli of soft, medium, and stiff polyacrylamide gels were measured using nanoindentation. The mean for all measurements is also shown on the graph. The y-axis has been log-transformed to demonstrate the order of magnitude differences between the stiffnesses.

A two-way ANOVA was performed in order to determine whether there was a difference in the elastic modulus measurements across different days and also between types of stiffness. The significance value (P-value) for the factor of day was 0.92, which means that the null hypothesis that there is not a significant difference in means between the measurements within the same stiffness group taken on different days cannot be rejected. This indicates that the modulus measurements are consistent across days, and that this result can be projected to all PA gels made with the same materials and protocol. The significance value for the factor of types of stiffness was 10^{-26}, which means that the null hypothesis that there is not a significant difference in measurements between gel stiffness types can be rejected. This indicates that the three levels of stiffness - soft, medium, and stiff – are different.

Changes in cytoskeletal morphology on substrates of different stiffnesses

In order to confirm the results of previous experiments that showed differences in cytoskeletal morphology on substrates of different stiffnesses, human foreskin fibroblasts (HFFs) were plated on PA gel substrates of three different stiffness (soft, medium, stiff), and their nuclei were stained with bisbenzimide, and cytoskeleton was stained with FITC phalloidin. An example of the resulting images can be seen in Figure 6. The DAPI, and FITC channels were merged in order to demonstrate the differences in cytoskeleton between cells on the three stiffnesses of gels. The HFFs on soft gels had a rounded morphology and were not as spread out compared to HFFs on the medium and stiff gels. The cells on the medium gels had more of a triangular shape, while the cells on stiff gels had an elongated shape.

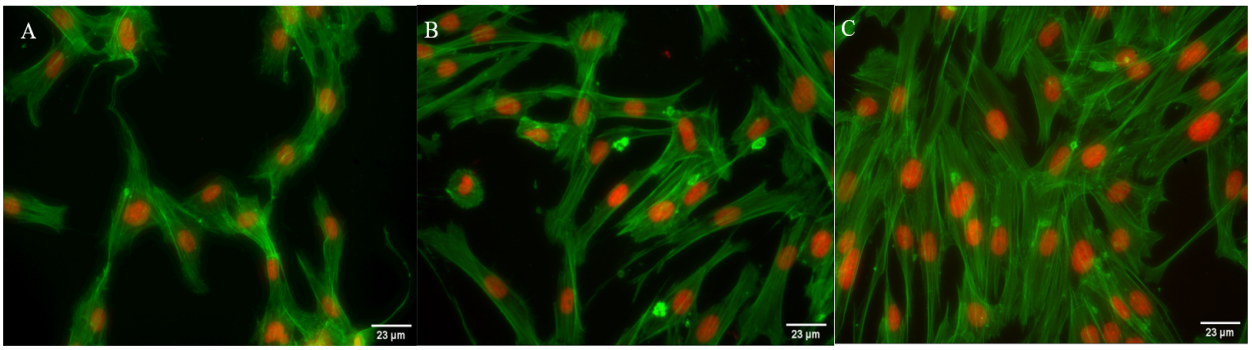

Figure 6. Cell morphology differs on substrates of different stiffnesses. Human foreskin fibroblasts (HFFs) were plated on collagen-coated polyacrylamide gels with varying stiffnesses. (A) is soft, ~1,000 Pa; (B) is medium, ~10,000 Pa; (C) is stiff, around ~100,000 Pa. The cells were fixed and the nuclei were stained with bisBenzamide (red) and actin was stained with FITC phalloidin (green). The cytoskeletal morphology differs across the three stiffnesses, with the cells on soft gels having an unspread morphology, not covering most of the gel surface, and having few F-actin stress fiber bundles, and the cells on stiff gels having a spread morphology, covering most of the gel surface, and having bundles of stress fibers. The cells on the medium gels were in between, with some having a morphology similar to those on the soft, and some having a morphology similar to those on the stiff.

Toxoplasma gondii invasion assays

Wild type parasites

Three invasion assay experiments were performed using wild type parasites and host cells on soft, medium, and stiff polyacrylamide gels and glass (Figure 7). The number of invaded parasites in ten fields of view was counted manually and with the automated counting workflow, although the numbers in Figure 7 reflect the manual counts. Due to time constraints, only two experiments using wild type parasites were able to be performed, so we could not use a one-way ANOVA to determine whether there was a significant difference between the mean number of invaded parasites on the four substrates. However, based on the trend of increased invasion as the stiffness of the substrate stiffness increases which is evident in Figure 7, we would expect that the one-way ANOVA would show that there is a significant difference between the means. This result would indicate that the ability of wild type *T. gondii* parasites to invade is dependent on the stiffness of the substrate that the host cells are plated on.

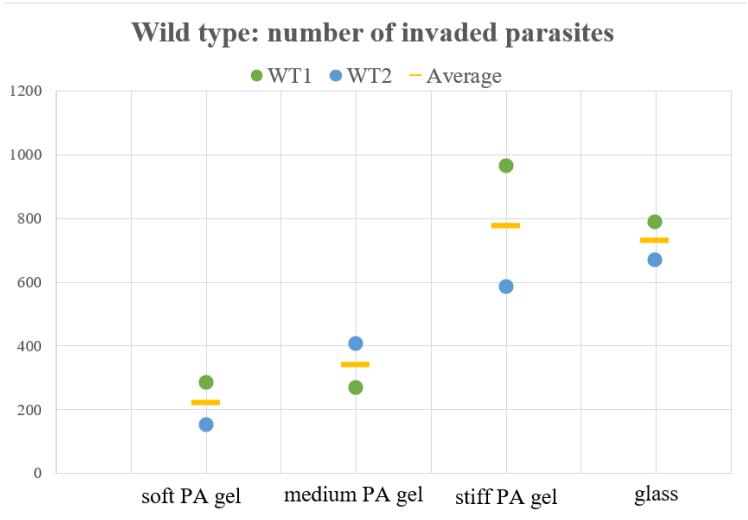

Figure 7. Results of wild type invasion assays
Three invasion assays were performed using wild type parasites and host cells on four types of substrates. The number of invaded parasites in ten fields of view is given by a circle symbol for each of the experiments (WT1, WT2) and each type of substrate (soft gel, medium gel, stiff gel, glass). The average of both experiments is also indicated on the graph with a line symbol.

The number of invaded wild type parasites for cells on glass substrates in our experiments was different from the number of invaded parasites for cells on glass substrates in other experiments in the literature. In Leung et al. (2017), the number of invaded parasites in 10 fields of view was 256 ± 29, while in Nagayasu et al. (2017) the number of invaded parasites in 15 fields of view was 2435 ± 84. We counted 728 ± 61 invaded wild type parasites for host cells on glass substrates. The two experiments from the literature used human foreskin fibroblasts to culture parasites and measure invasion, which we also used. Our measured invasion rate is within the range of the invasion measured by Leung et al. and Nagayasu et al., which serves to validate our results.

Triple knockout parasites

Three invasion assay experiments were performed using triple knockout parasites and host cells on soft, medium, and stiff polyacrylamide gels and glass (Figure 8). The number of invaded parasites in ten fields of view was counted manually and with the automated counting workflow. A one-way ANOVA was run in order to determine whether the mean number of invaded parasites was statistically significantly different between the four types of substrate. The resulting P-value of 0.06 was higher than the significance level of 0.05, meaning that the null hypothesis that the means are equal cannot be rejected. This indicates that it is possible that the triple knockout proteins, SPM1, TLAP2, and TLAP3, may be involved in host cell cytoskeleton dependent invasion. However, the large variance in the number of invaded parasites between experiments may be affecting the result of the ANOVA. Therefore, more experiments would need to be performed in order to increase the power of the significance test.

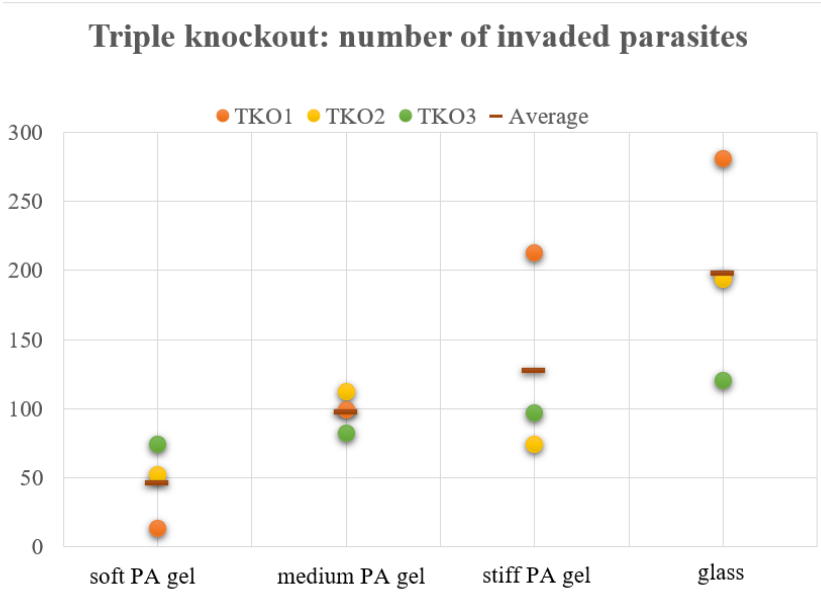

Figure 8. Results of triple knockout invasion assays
Three invasion assays were performed using triple knockout parasites and host cells on four types of substrates. The number of invaded parasites in ten fields of view is given by a circle symbol for each of the experiments (TKO1, TKO2, TKO3) and each type of substrate (soft gel, medium gel, stiff gel, glass). The average of all three experiments is also indicated on the graph with a line symbol.

The decreased invasion of the TKO parasites compared to wild type parasites was consistent with the literature. Liu et al. measured the number of plaques formed by TKO parasites and found it to be 24% of the number of plaques formed by wild type parasites. We found that the number of invaded TKO parasites was 27% of the number of wild type parasites for host cells plated on glass substrates. Although the number of plaques formed and the number of invaded parasites are not the same measurement, they both measure invasion and therefore can be compared.

Automated cell counting

The automated cell counting workflow was first run on a set of five test images, each of which had 195 objects. The images were created through a Matlab code, which created two stacked scatter plots made from a randomized set of 100 coordinates. The first scatter plot used bright green markers, while the second scatter plot used slightly dimmer green markers, made to mimic less fluorescent parasites in an actual image. Lastly, the background of the plot was changed to black to better match that of an experimental image. The workflow was also run on five sets of FITC and TRITC fluorescent images collected from invasion assays. Paired t-tests were performed for the test, FITC, and TRITC images comparing manual counts to automatic counts, and P-values of 0.556, 0.348, and 0.188 were calculated, respectively. These P-values are all greater than the significance level of 0.05, indicating that the difference between the means of the manual and automatic counts is not statistically significant. Therefore, we can conclude that our automated counting workflow is as accurate as manual counting, and that the workflow can be used with confidence to analyze the results of future invasion assays.

Discussion

Polyacrylamide gel production and testing

Polyacrylamide gels are a type of 2D hydrogel substrate and are simple to produce, relatively cheap, and tunable to specific stiffnesses by modifying the relative concentrations of acrylamide and bis crosslinker. The stiffness in terms of elastic modulus was quantified using nanoindentation, and the values measured can be compared to the literature to confirm that our gel formulations are accurate. The elastic moduli we measured can be compared to values from a paper by Yeung et al., whose protocol for making polyacrylamide gels we adapted and used. Yeung et al. measured stiffness in terms of a shear modulus, G, which can be converted to elastic modulus, E, using the formula $E = 2G(1 + \upsilon)$ where ν is the Poisson's ratio and can be assumed to be about 0.5 (Chippada et al., 2010)**.** We can compare our measurements of modulus to their measurements on gels with the same percent of acrylamide and bis-acrylamide. They measured a soft PA gel with 0.06% bis crosslinker and 3% acrylamide to have an elastic modulus of around 600 Pa, while our measured elastic modulus for this formulation was 919.5 ± 266 Pa. Our medium gel, with 0.3% bis crosslinker and 5% acrylamide, had an elastic modulus of 14,508 ± 3,691 Pa while theirs was around 6,000 Pa. Finally, our stiff gel with 0.6% bis crosslinker and 10% acrylamide had a measured modulus of 108,554 ± 27,754 Pa and theirs had an estimated modulus of 600,000 Pa. One reason for the discrepancy between the expected and measured values is that the Poisson's ratio may actually be greater or less than 0.5 for our polyacrylamide gels. Another reason is that the expected moduli were read off of a chart, which is less accurate than having the original data points. However, our measured elastic moduli are within the same magnitudes of the expected values. Our important finding is that we can formulate gels to have stiffnesses that are an order of magnitude apart from each other, which allows us to examine host cell cytoskeletal morphology in significantly diverse environments.

The reason the range of stiffnesses for the polyacrylamide gels was chosen is that their elastic moduli are similar to that of the extracellular matrix (ECM), to which cells attach. The ECM and other cells have elastic moduli on the order of 10 to 10,000 Pa (Wakatsuki et al., 2000).

Invasion assays

The results of the ANOVA comparing invasion on the four substrates indicate that these three proteins may be involved in host cell cytoskeleton dependent invasion, as the P-value of 0.06 was greater than the chosen significance level of 0.05. However, this P-value is relatively close to the significance level and the large variance between data points within a treatment may contribute to this large P-value. Therefore, more invasion assay experiments using triple knockout parasites must be performed in order to determine whether the results from the first three experiments are accurate. If, when further experiments are performed, the P-value of the ANOVA is significant, meaning that there is a significant difference between means, we can conclude that the triple knockout proteins are not involved in host cell cytoskeleton dependent invasion. Therefore, the next step would be to perform invasion assays using

mutant parasites with other proteins knocked out. One mutant that has been shown to have decreased invasion capabilities using cells on glass substrates is a knockout of KinesinA and APR1, which are proteins that stabilize the apical polar ring and microtubule array (Leung et al., 2017). Another mutant has the DCX protein knocked out, and experiments have shown that this protein stabilizes conoid fibers and is involved in invasion (Nagayasu et al., 2017). A pattern of invasion that differs from what is seen using wild type parasites would indicate that these proteins are involved in invasion that is dependent on the cytoskeletal morphology of the host cell.

Knowing which proteins are involved in *T. gondii* invasion is important for the development of treatment for toxoplasma infection and toxoplasmosis. A drug that targets these proteins could prevent parasites from invading. Many of these proteins are also important for replication, so targeting them could prevent the parasites from multiplying even when already in the tissue. Learning about proteins involved in *T. gondii* invasion could also give insight into the invasion mechanisms of *Plasmodium*, the parasite that causes malaria. *T. gondii* and *Plasmodium* are in the same phylum and share several proteins and structures.

Automated segmentation workflow

As shown above, the automated counting workflow that we developed is at least as accurate as manual counting and requires much less time and effort. By comparing the results of the automated counting to manual counting and a test dataset, we can be confident that the automated counting will produce accurate results and can therefore be used on datasets that are collected in the future. The method of semiautomated counting that is described by Yeung et al. in their paper from which we sourced the protocol for the invasion assay utilized ImageJ/FIJI. They thresholded using an Otsu algorithm to create a binarized image and then separated the objects with watershed separation. They used a size filter to exclude objects too large or small to be parasites and then counted the objects. This method was not suitable for our dataset because the parasites in the images did not have a consistent intensity, which would have impacted thresholding. In addition, our images had a lot of fluorescence that was not from the parasites due to issues with non-specific antibody binding, so we could not be certain that every fluorescent object in the images was actually a parasite. Manually counting the parasites in the image was another option for analyzing the results of the invasion assays. However, with hundreds of images generated per experiment and dozens of parasites per image, this method is costly in terms of time and effort. Therefore, it was necessary to create a method of automated counting which could produce accurate results with less labor involved. CellProfiler was chosen for the automated counting because it allows for the creation of an image analysis pipeline by picking modules and putting them in a specified order. This meant that we did not have to combine different software programs in our workflow and that the process is faster and easier to use. Although our workflow is demonstrated to be accurate when compared to manual counts, there are certain aspects that could be improved. The workflow is not good at detecting two parasites that are touching, and they must often be separated manually. Additionally, the parasites have a distinct banana shape that distinguishes them from autofluorescence in the images, but the workflow is not able to make the distinction. Fixing these problems would lead to more accurate results that require less time and effort to obtain.

Limitations of cell type

The parasite enters the host through the intestinal tract by ingestion of parasite-containing material. So, the gut epithelial cell layer is one of the primary locations in which invasion occurs. Our experiments use fibroblasts instead of epithelial cells, so the results cannot be directly compared to the *in vivo* environment in which invasion would occur. In literature to model the intestinal epithelial barrier, the Caco-2 cell line is used, which is an immortalized cell line of human colorectal adenocarcinoma cells (Briceño et al., 2016). HFFs can propagate indefinitely under the appropriate care, which better suits the scope of the experiment both in terms of time limitations and material availability. Current literature on *T. gondii* invasion assays has used both fibroblasts and epithelial cells, but toxoplasmosis is known to occur in a variety of nucleated cells in the body. We cannot yet translate the data from this study into

conclusions on what the result would be if the same experiments were performed with epithelial cells, but we predict that we would observe similar trends in invasion rates corresponding with both parasitic protein expression and cytoskeleton stiffness.

References

Briceño, M. P., Nascimento, L. A. C., Nogueira, N. P., Barenco, P. V. C., Ferro, E. A. V., Rezende-Oliveira, K., Goulart, L. R., Alves, P. T., Barbosa, B. de F., Lima, W. R., & Silva, N. M. (2016). Toxoplasma gondii Infection Promotes Epithelial Barrier Dysfunction of Caco-2 Cells. *Journal of Histochemistry and Cytochemistry*, *64*(8), 459–469. https://doi.org/10.1369/0022155416656349

CDC - Toxoplasmosis. (2021, January 15). https://www.cdc.gov/parasites/toxoplasmosis/index.html

Chippada, U., Yurke, B., & Langrana, N. A. (2010). Simultaneous determination of Young's modulus, shear modulus, and Poisson's ratio of soft hydrogels. *Journal of Materials Research*, *25*(3), 545–555. https://doi.org/10.1557/JMR.2010.0067

Discher, D. E., Janmey, P., & Wang, Y. (2005). Tissue Cells Feel and Respond to the Stiffness of Their Substrate. *Science*, *310*(5751), 1139–1143. https://doi.org/10.1126/science.1116995

Dobrowolski, J. M., & Sibley, L. D. (1996). Toxoplasma Invasion of Mammalian Cells Is Powered by the Actin Cytoskeleton of the Parasite. *Cell*, *84*(6), 933–939. https://doi.org/10.1016/S0092-8674(00)81071-5

Guérin, A., Corrales, R. M., Parker, M. L., Lamarque, M. H., Jacot, D., El Hajj, H., Soldati-Favre, D., Boulanger, M. J., & Lebrun, M. (2017). Efficient invasion by Toxoplasma depends on the subversion of host protein networks. *Nature Microbiology*, *2*(10), 1358–1366. https://doi.org/10.1038/s41564-017-0018-1

Hill, D. E., & Dubey, J. P. (2018). Toxoplasma gondii. In Y. R. Ortega & C. R. Sterling (Eds.), *Foodborne Parasites* (pp. 119–138). Springer International Publishing. https://doi.org/10.1007/978-3-319-67664-7_6

Leung, J. M., He, Y., Zhang, F., Hwang, Y.-C., Nagayasu, E., Liu, J., Murray, J. M., & Hu, K. (2017). Stability and function of a putative microtubule-organizing center in the human parasite Toxoplasma gondii. *Molecular Biology of the Cell*, *28*(10), 1361–1378. https://doi.org/10.1091/mbc.e17-01-0045

Liu, J., He, Y., Benmerzouga, I., Sullivan, W. J., Morrissette, N. S., Murray, J. M., & Hu, K. (2016). An ensemble of specifically targeted proteins stabilizes cortical microtubules in the human parasite Toxoplasma gondii. *Molecular Biology of the Cell*, *27*(3), 549–571. https://doi.org/10.1091/mbc.e15-11-0754

Montoya, J. G., & Contopoulos-Ioannidis, D. (2021). Toxoplasmosis. In J. E. Weatherhead (Ed.), *Neglected Tropical Diseases—North America* (pp. 69–91). Springer International Publishing. https://doi.org/10.1007/978-3-030-63384-4_5

Nagayasu, E., Hwang, Y.-C., Liu, J., Murray, J. M., & Hu, K. (2017). Loss of a doublecortin (DCX)-domain protein causes structural defects in a tubulin-based organelle of Toxoplasma gondii and impairs host-cell invasion. *Molecular Biology of the Cell*, *28*(3), 411–428. https://doi.org/10.1091/mbc.E16-08-0587

Ryning, F. W., & Remington, J. S. (1978). Effect of cytochalasin D on Toxoplasma gondii cell entry. *Infection and Immunity*, *20*(3), 739–743.

Silva, C. V. da, Silva, E. A. da, Cruz, M. C., Chavrier, P., & Mortara, R. A. (2009). ARF6, PI3-kinase and host cell actin cytoskeleton in Toxoplasma gondii cell invasion. *Biochemical and Biophysical Research Communications*, *378*(3), 656–661. https://doi.org/10.1016/j.bbrc.2008.11.108

Solon, J., Levental, I., Sengupta, K., Georges, P. C., & Janmey, P. A. (2007). Fibroblast Adaptation and Stiffness Matching to Soft Elastic Substrates. *Biophysical Journal*, *93*(12), 4453–4461. https://doi.org/10.1529/biophysj.106.101386

Wakatsuki, T., Kolodney, M. S., Zahalak, G. I., & Elson, E. L. (2000). Cell mechanics studied by a reconstituted model tissue. *Biophysical Journal*, *79*(5), 2353–2368.

Yeung, T., Georges, P. C., Flanagan, L. A., Marg, B., Ortiz, M., Funaki, M., Zahir, N., Ming, W., Weaver, V., & Janmey, P. A. (2005). Effects of substrate stiffness on cell morphology, cytoskeletal structure, and adhesion. *Cell Motility*, *60*(1), 24–34. https://doi.org/10.1002/cm.20041